



INEEL/CON-02-01206
PREPRINT

**Preliminary Results Of A High-Resolution
Aeromagnetic Survey To Identify Buried Faults
At Dixie Valley, Nevada**

**R. P. Smith
V. J. S. Grauch
D. D. Blackwell**

September 22, 2002

Geothermal Resources Council Annual Meeting

This is a preprint of a paper intended for publication in a journal or proceedings. Since changes may be made before publication, this preprint should not be cited or reproduced without permission of the author.
This document was prepared as a account of work sponsored by an agency of the United States Government. Neither the United States Government nor any agency thereof, or any of their employees, makes any warranty, expressed or implied, or assumes any legal liability or responsibility for any third party's use, or the results of such use, of any information, apparatus, product or process disclosed in this report, or represents that its use by such third party would not infringe privately owned rights. The views expressed in this paper are not necessarily those of the U.S. Government or the sponsoring agency.

Preliminary Results of a High-Resolution Aeromagnetic Survey to Identify Buried Faults at Dixie Valley, Nevada

R.P. Smith¹, V.J.S. Grauch², and D.D. Blackwell³

¹Idaho National Engineering and Environmental Laboratory, Idaho Falls, ID 83401-2107

²U.S. Geological Survey, MS 964, Federal Center, Denver, CO 80225

³Department of Geological Sciences, Southern Methodist University, Dallas, TX 75175

Key Words

High-resolution aeromagnetic survey, Dixie Valley, faults, structure, mapping

Abstract

Preliminary results from a high-resolution aeromagnetic survey (200m line spacing) acquired in Dixie Valley early in 2002 provide confirmation of intra-basin faulting based on subtle surface indications. In addition the data allow identification of the locations and trends of many faults that have not been recognized at the surface, and provide a picture of intrabasin faulting patterns not possible using other techniques. The data reveal a suite of northeasterly-trending curving and branching faults that surround a relatively coherent block in the area of Humboldt Salt Marsh, the deepest part of the basin. The producing reservoir occurs at the north end of this coherent block, where rampart faults from the northwest side of the valley merge with antithetic faults from the central and southeast parts of the valley.

Introduction and Methods

Recent geologic mapping focused on fault distribution near the producing geothermal reservoir in Dixie Valley and relied on subtle surface features (small scarps, small graben, linear alignments of springs, vegetation and color lineaments) to define fault locations beneath and within the intrabasin sediments (Smith et al, 2001). In order to increase confidence in the locations of buried faults a high-resolution aeromagnetic survey was conducted over a 940 km² area. The area extends from Dixie Meadows northeastward to the Sou Hills, and from the eastern front of the Stillwater Range to the western edge of the Clan Alpine Range (Figure 1) and includes almost all of the area in which the recent geologic mapping was done.

Parameters for the high-resolution aeromagnetic survey (Table 1) are similar to those for other surveys which have provided information on the distribution of buried faults in basin-fill sediments (Grauch, 2001; Grauch et al., 2001; Grauch and Millegan, 1998). The main distinguishing feature of this survey is the extreme topographic relief at the east front of the Stillwater Range, which dictated the use of a helicopter to acquire data near the range-front fault. Detailed descriptions of the procedures followed for data acquisition and processing are contained in U. S. Geological Survey and PRJ, Inc. (in press).

Table 1. Specifications of the Dixie Valley high-resolution aeromagnetic survey (2002)

Dates of Acquisition	January 20 – February 2, 2002
Line Spacing	200 m, lines trend NW – perpendicular to regional structures
Tie lines	1000 m, lines trend NE – parallel to regional structures
Observation height above ground (average)	120 m
Instrument/Aircraft	Cesium-vapor magnetometer with sampling rate of 0.1 seconds towed below a Bell Jet Ranger helicopter
Area Surveyed	~940 km ²
Total flight-line length	5740 line km

After data processing to remove diurnal effects, noise, and the Earth's magnetic field, the total-field aeromagnetic data were gridded at a 50-m interval (Figure 2). Preliminary analysis focused on enhancing the signature of shallow faults in the aeromagnetic data by using the gradient window method (Grauch and Johnston, in press), a modification of the horizontal-gradient method. The horizontal-gradient method (Cordell and Grauch, 1985; Blakely and Simpson, 1986) is based on a principle from gravity methods that steep gradients occur over near-vertical contacts between units with differing physical properties. For magnetic data, the same principle can be applied after transforming the data into a form that is mathematically similar to gravity data, called pseudogravity (Baranov, 1957). Local peaks (or ridges) in the magnitude of the horizontal gradient of pseudogravity give the locations of steepest gradients, intuitively similar to taking the first derivative of a curve. A modification of the method, which isolates the horizontal-gradient magnitudes associated with short-wavelength anomalies (Grauch and Johnston, in press), was applied to the Dixie Valley data after transforming to pseudogravity (Figure 3). Future study will include analyses to estimate the depths and refine map locations of faults with respect to anomalies visible on the map.

Fault Patterns Indicated by Aeromagnetic Anomalies and Geologic Mapping in Dixie Valley

The total-field aeromagnetic map (Figure 2) shows the same gross features as earlier, low-resolution aeromagnetic maps (Smith, 1968; Thompson et al., 1967). Notably, the patterns of major positive and negative aeromagnetic anomalies are similar; the large positive anomalies have been interpreted to represent large bodies of mafic rocks in the basement beneath the valley fill sediments or horst blocks of mafic basement rocks within the valley.

In addition to the large positive and negative anomalies, the map (Figure 2) shows a suite of northeast-trending, short wave-length, linear anomalies which have been emphasized by the narrow ridges in the horizontal gradient map (Figure 3). Many of the linear anomalies are continuous for 10 or more km, and commonly show branching and curving shapes. In addition, a group of short wavelength negative anomalies (dimples) present in the area of Hyder Hot Springs may represent altered areas where magnetic minerals have been destroyed along plumbing pathways that feed the hot springs. Alternatively, the negative anomalies may be due to buried, extinct vents related to Tertiary volcanic rocks that have reverse-polarity remanent magnetization (Hudson and Geissman, 1991). In areas where bedrock is exposed at the surface (along the northwestern edge and the central part of the southeastern edge of the surveyed area) the pattern of anomalies is much rougher than in areas covered with thick alluvial sediments.

Superposition of mapped faults (Smith et al., 2001; Whitney, 1980; Thompson et al., 1967) onto the horizontal gradient map shows that many of the short wavelength, linear magnetic anomalies have a close correspondence to the mapped fault traces (Figure 4). The correspondence is identical to that in the Albuquerque Basin where “the linear anomalies have become important geologic mapping tools that are used to connect and extend isolated exposures of faults, to confirm ambiguous surface evidence of faults, to infer buried faults, and to pinpoint areas to look for fault evidence on the ground” (Grauch 2001; Grauch et al., 2001). After extensive investigations of possible sources of the linear anomalies in the Albuquerque Basin, Grauch et al (2001) show that they are explained by fault offsets that juxtapose sediment layers of differing magnetic properties, and that they represent offsets that occur within the upper 500-600 meters of the valley-fill sediments.

The close correspondence of mapped faults in Dixie Valley to narrow ridges in the horizontal gradient map (Figure 4) suggests that the aeromagnetic data can be used to extend the knowledge of faulting within the basin-fill sediments. By using the horizontal-gradient map (Figure 3) to infer the traces of faults we develop a more complete map of fault distribution in the valley (Figure 5). Faults can be interpreted from the horizontal-gradient magnitude by following the ridges in the horizontal-gradient magnitude map (Figure 3). This interpretation can be somewhat subjective, because peak magnitudes can also follow lithologic contacts, abrupt variations in magnetic properties within one rock unit, and steep basement relief. In contrast, the absence of linear magnetic anomalies does not necessarily imply the absence of faults; a lack of contrast in magnetic properties of the materials juxtaposed at the fault or minor offset along the fault could preclude aeromagnetic detection (Grauch et al., 2001).

The complete pattern of shallow faults (Figure 5) shows that faults with a strong surface expression also have a strong aeromagnetic signal, that there are many faults in the valley that exhibit no surface expression, and that some of the faults with surface expression are sections of longer faults.

Interpretation of Fault Patterns in Dixie Valley

Intrabasin faults in Dixie Valley trend generally northeast, subparallel to the range front fault (Figure 5), but they commonly exhibit curving and branching shapes. Notably, the Buckbrush fault system, a major intrabasin system with numerous springs localized along its trace, broadens and branches in a classic “horsetail” fashion just south of Humboldt Salt Marsh. This suggests that it terminates to the south of the mapped area and that displacement is transferred to nearby faults to the east or west. There is a tendency for all the faults, including the exposed range-front fault to turn to a more easterly direction at the north end of Dixie Valley, in the Sou Hills-Hyder Hot Springs area. The mapped range-front fault and several faults inferred from aeromagnetic anomalies in the northeastern part of the area turn quite abruptly eastward, indicating a significant change in fault geometry at the northern end of the valley.

The inferred presence of a buried synthetic rampart fault just outboard of the range-front fault is strengthened by the aeromagnetic anomalies present there. The aeromagnetic signature is especially convincing in the northern part of the area between the geothermal field and the Sou Hills (Figure 4). Along the western side of the valley near the geothermal field, faults inferred

from the aeromagnetic data (Figure 5) are supported by gravity and geologic mapping (Blackwell et al., 1999, 2000; Smith et al., 2001) and confirmed by recent drilling. At the southern end, near Dixie Meadows, the horizontal gradient anomaly and the steepest part of the gravity gradient (Blackwell et al. 1999; Smith et al., 2001) are coincident, and lie outboard of the Dixie Meadows graben system. This suggests a moderate eastward dip for the rampart fault, unlike the areas in the vicinity of the deep wells 36-14 and 45-14 where drilling shows that the fault is essentially vertical. It is clear that the extension that produced the Dixie Meadows graben system is thin-skinned basin-ward sliding of alluvial fan material on saturated fine-grained sediments of the salt marsh (Caskey et al., 2000; Smith et al, 2001), and therefore does not necessarily owe its existence to surface displacement along a deep rampart fault. However, the close spatial correlation of the gravity and magnetic gradients reflect the presence of a deeper structure whose surface expression could control the location of the graben system

The only part of the basin without surface or aeromagnetic evidence of intrabasin faulting is the area in and around the Humboldt Salt Marsh. This seems to be the deepest part of the basin, flanked on both sides by intrabasin fault systems that downdrop the central block. The geothermal field is located at the north end of this deep, coherent block, where its flanking fault systems merge. The area of merging is also marked by an abundance of springs and flowing wells, suggesting that a number open fault systems occur here, extending from the deep bedrock, where they provide space for the geothermal fluids, into near-surface sediments, where they allow rise of water from artesian aquifers near the surface.

Conclusions and Recommendations

This is a test of high-resolution aeromagnetic surveys in basins other than the Albuquerque Basin, where the technique was first demonstrated. There was some early concern that the deep, narrow basin geometry, the extremely steep front of the Stillwater Range, and the presence of very magnetic mafic rocks in the bedrock in Dixie Valley would limit the usefulness of the technique here. But the data have proven to reveal the intra-basin fault pattern with unexpected clarity. The data allow identification of the positions and attitudes of numerous faults that have no surface expression, and provide a geometric relationship of the geothermal field to the fault pattern that will aid further geothermal exploration in the area. As additional processing and filtering of the data are performed, the fault pattern will be refined, and the relationship of deep to shallow aeromagnetic signatures of faulting will be further clarified.

This effort has shown that topographic constraints on aeromagnetic data acquisition can be overcome by use of helicopter flight platforms, and that the method can provide useful data in basins where bedrock composition and basin geometry are not ideal. This is a technique that may prove useful for geothermal exploration, structural investigations, and groundwater problems in many sediment-filled basins of extensional environments.

Acknowledgements. Funding for this work was provided by the U.S. Department of Energy, Office of Geothermal and Wind Technologies, under Contract DE-AC07-99ID13727.

References

Baranov, V. (1957) A new method for interpretation of aeromagnetic maps--pseudogravity anomalies; *Geophysics*, v. 22, p. 359-383.

- Blackwell, D.D., Wisian, K.W., Benoit, D., and Gollan, B. (1999) Structure of the Dixie Valley Geothermal System, a "Typical" Basin and Range Geothermal System, From Thermal and Gravity Data; Geothermal Resources Council Transactions, v.23, p.525-531.
- Blackwell, David D., Golan, Bobbie, and Benoit, Dick (2000) Thermal regime in the Dixie Valley Geothermal System; Geothermal Resources Council Transactions, v.24, p.223-228.
- Blakely, R. J., and Simpson, R. W. (1986) Locating edges of source bodies from magnetic or gravity anomalies; Geophysics, v. 51, p. 1494-1498.
- Caskey, S.J., Bell, J.W., Slemmons, D.B., and Rameli, A.R. (2000) Historical surface faulting and paleoseismology of the central Nevada seismic belt; in Lageson, D.R., Peters, S.G., and Lahren, M.M., editors, Great Basin and Sierra Nevada: Geological Society of America Field Guide 2, p23-44.
- Cordell, Lindrith, and Grauch, V. J. S. (1985) Mapping basement magnetization zones from aeromagnetic data in the San Juan Basin, New Mexico; in Hinze, W. J., editor, The utility of regional gravity and magnetic maps: Society of Exploration Geophysicists, p. 181-197.
- Grauch, V J S (2001) High-resolution aeromagnetic data, a new tool for mapping intrabasinal faults; example from the Albuquerque Basin, New Mexico: Geology, v.29, pp.367-370.
- Grauch, V.J.S., and Millegan, P. S., 1998, Mapping intrabasinal faults from high-resolution aeromagnetic data: The Leading Edge, v.17, p.53-55.
- Grauch, V.J.S.; Hudson, M.R., Minor, S.A. (2001) Aeromagnetic expression of faults that offset basin fill, Albuquerque Basin, New Mexico; Geophysics, v.66, p.707-720.
- Grauch, V.J.S., and Johnston, C.S. (in press) Gradient window method: A simple way to isolate regional from local horizontal gradients in potential-field gridded data: 72nd Annual International Meeting, Society of Exploration Geophysicists, Expanded Abstracts, in press.
- Hudson, M. R., and Geissman, J.W. (1991) Paleomagnetic evidence for the age and extent of middle Tertiary counterclockwise rotation, Dixie Valley region, west central Nevada: Journal of Geophysical Research, v. 96, no. B3, p. 3979-4006.
- Smith, R.P., Wisian, K.W., and Blackwell, D.D. (2001) Geologic and Geophysical Evidence for Intra-basin and Footwall Faulting at Dixie Valley, Nevada; Geothermal Resources Council Transactions, v. 25, p. 323-326.
- Smith, T.E. (1968) Aeromagnetic measurements in Dixie Valley, Nevada; Implications on Basin-Range structure; Journal of Geophysical Research, v.73, p.1321-1331.
- Thompson, G.A., Meister, L.J., Herring, A.T., Smith, T.E., Burke, D.B., Kovach, R.L., Burford, R.O., Salehi, I.A., and Wood, M.D. (1967) Geophysical study of Basin-Range structure, Dixie Valley region, Nevada; Air Force Cambridge Research Laboratory, Report No. 66-848.
- U. S. Geological Survey and PRJ, Inc. (in press) Description of digital aeromagnetic data collected over Dixie Valley, Churchill and Pershing Counties, Nevada: U. S. Geological Survey Open-File Report 02-.
- Whitney, R.A. (1980) Structural-Tectonic analysis of northern Dixie Valley, Nevada; Masters Thesis, University of Nevada, Reno.

Figure Captions

Figure 1. Location and Index map

Figure 2. Shaded-relief image of total-field aeromagnetic data, illuminated from the northwest.

Figure 3. Shaded-relief image of the horizontal-gradient magnitude of gradients associated with local (shallow) features, computed after transformation of the aeromagnetic data to pseudogravity and application of the gradient window method (Grauch and Johnston, in press) using the residual in a 1 X 1 km moving window. Illumination from the northwest.

Figure 4. Horizontal Gradient Magnitude (HGM) map (Figure 3) with mapped faults superimposed.

Figure 5. The complete distribution of shallow faults as indicated by surface mapping and high-resolution aeromagnetic anomalies. Selected deeper faults are also inferred from aeromagnetic anomalies along the western range front and from seismic profiles.

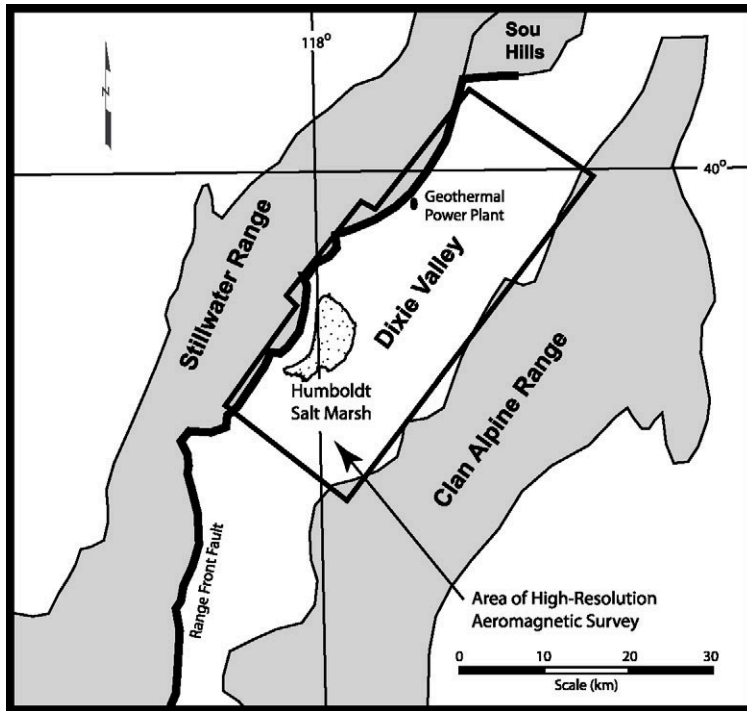


Figure 1. Index map showing the area of the high-resolution aeromagnetic survey.

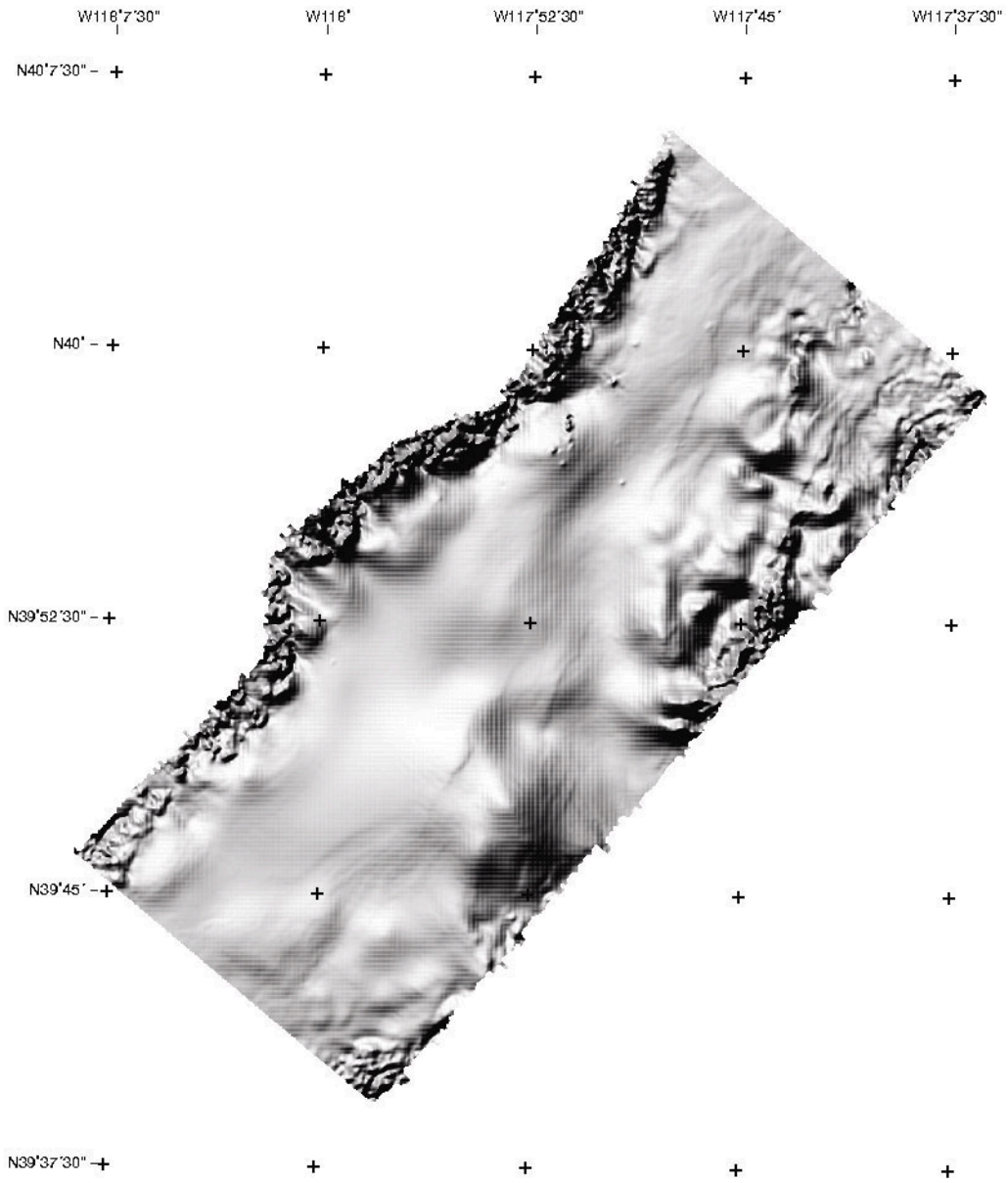


Figure 2. Shaded relief map of total field raw aeromagnetic data for the survey area in Dixie Valley.

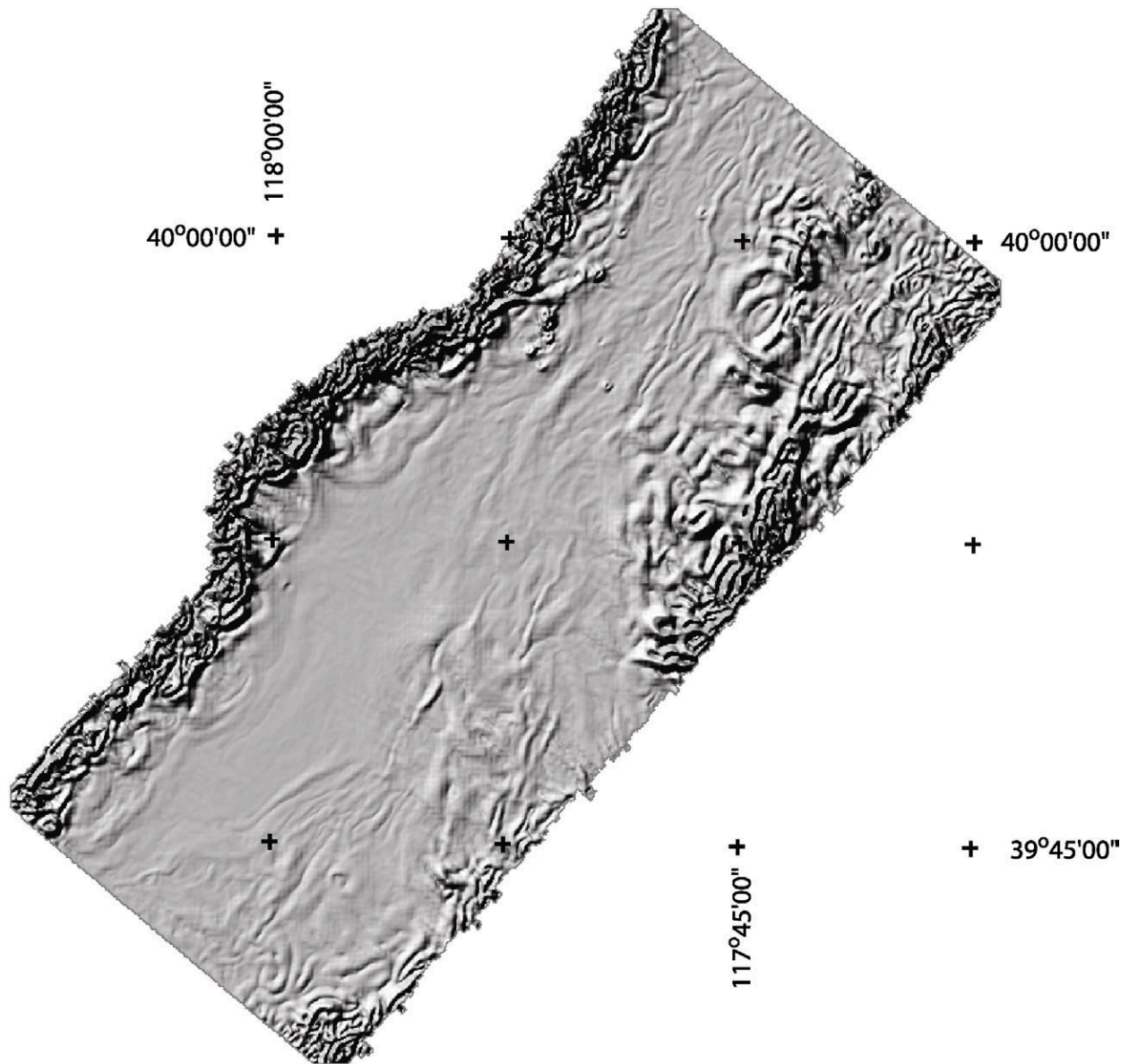


Figure 3. Shaded-relief image of the horizontal-gradient magnitude of gradients associated with local (shallow) features, computed after transformation of the aeromagnetic data to pseudogravity and application of the gradient window method (Grauch and Johnston, in press) using the residual in a 1 X 1 km moving window. Illumination from the northwest.

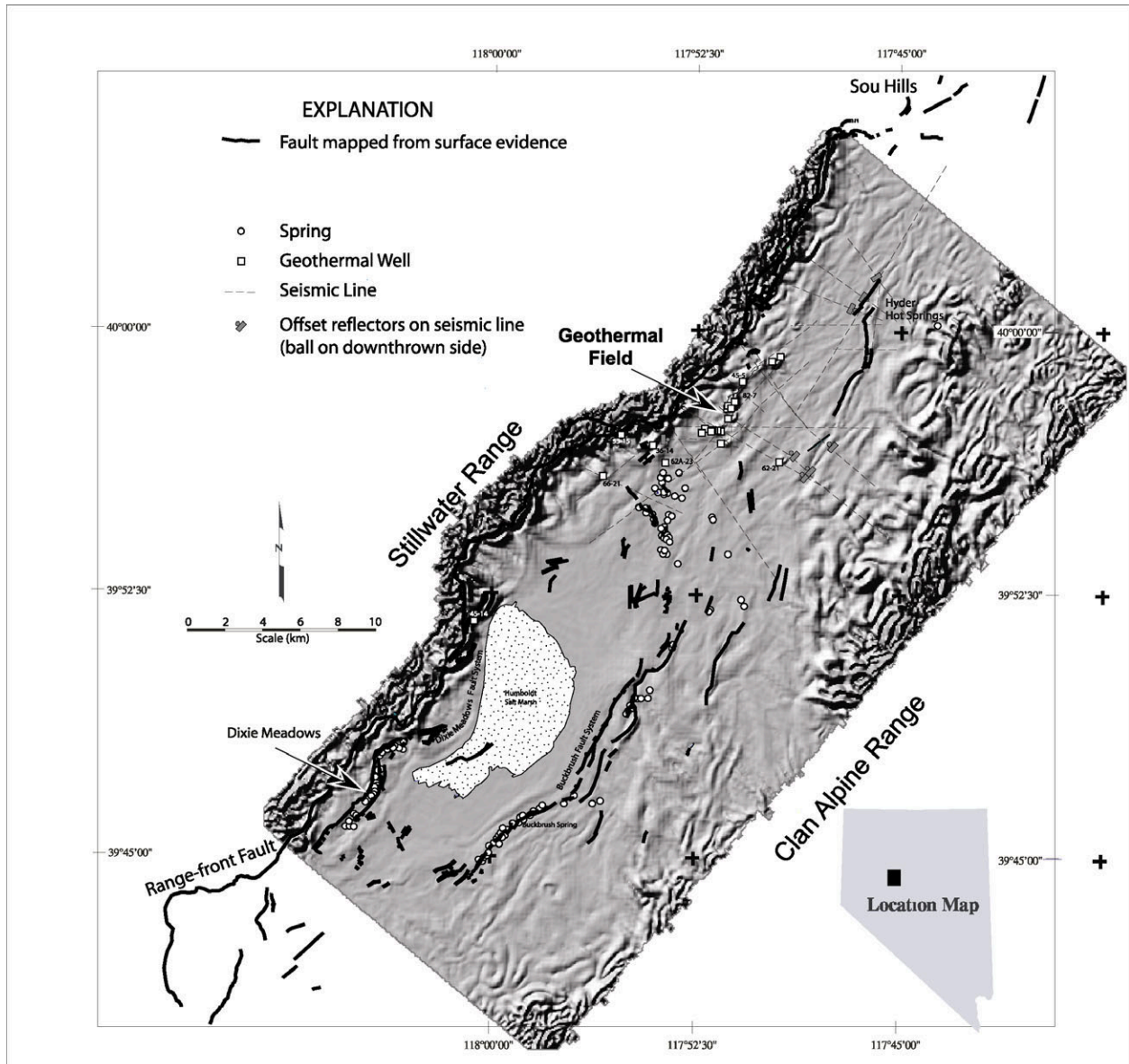


Figure 4. Horizontal Gradient Magnitude (HGM) map (Figure 3) with mapped faults superimposed..

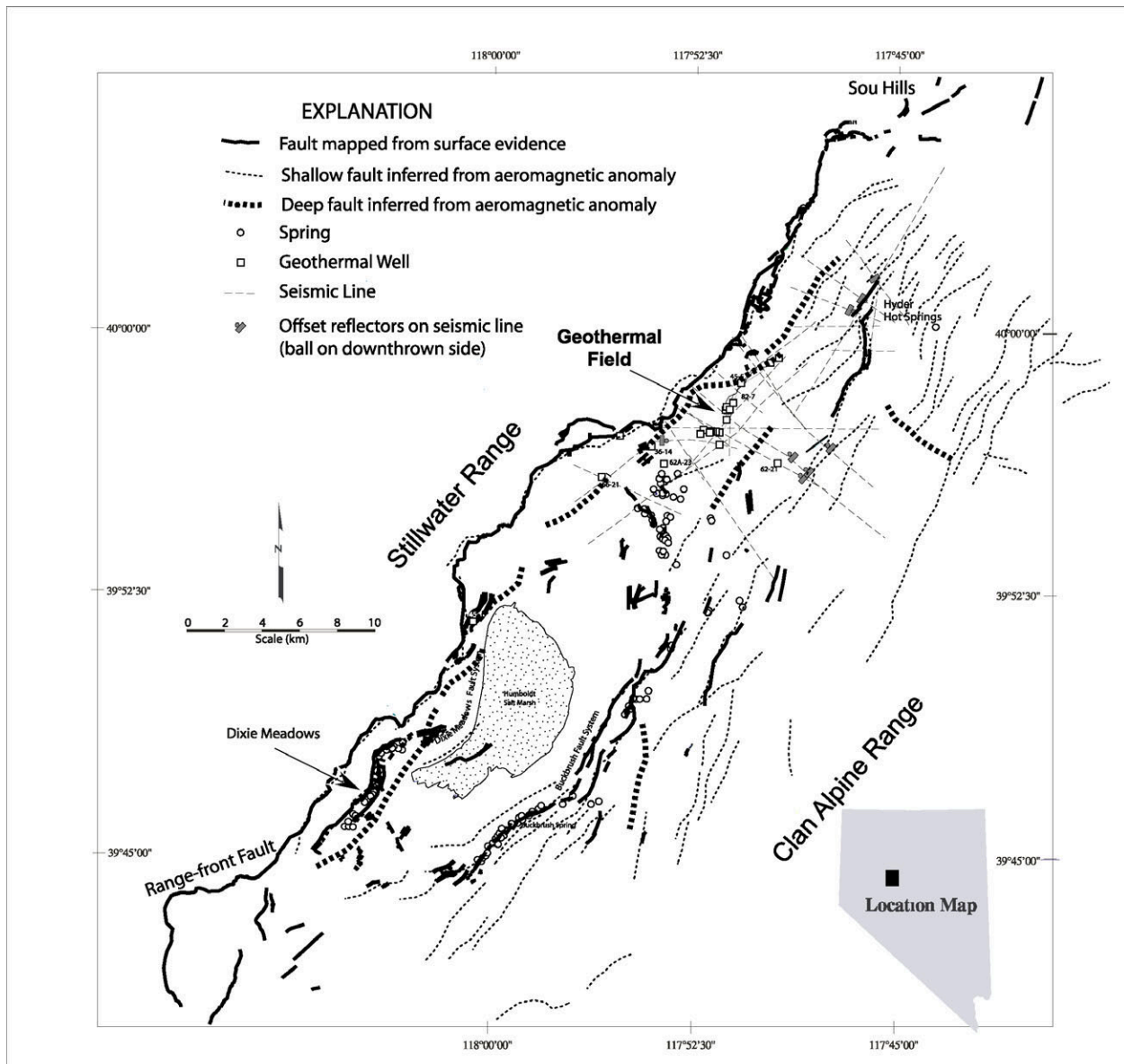


Figure 5. The complete distribution of shallow faults as indicated by surface mapping and high-resolution aeromagnetic anomalies. Selected deeper faults are also inferred from aeromagnetic anomalies along the western range front and from seismic profiles.